LOGISTICAL AND ANALYTICAL APPROACH TO A FAILURE ABOARD THE INTERNATIONAL SPACE STATION

Steve McDanels, M. Clara Wright, Victoria Salazar, David Lubas, Bryan Tucker
National Aeronautics and Space Administration (NASA)
Kennedy Space Center, Florida

Abstract
The starboard Solar Alpha Rotary Joint (SARJ) from the International Space Station (ISS) began exhibiting off-nominal electrical demands and vibration. Examination by spacewalking astronauts revealed metallic debris contaminating the system and damage to the outboard race of the SARJ. Samples of the contamination were returned to Earth and analyzed. Excessive friction caused the nitride region of the 15-5 PH stainless steel race to spall, generating the debris and damaging the race surface. Excessive vibration and excess power was required to operate the system as a result.

Key Words
Failure Analysis, Spalling, International Space Station

Background
One of the most formidable failure investigations performed in conjunction with NASA at the Kennedy Space Center would be the investigation of the failure of a Solar Alpha Rotary Joint (SARJ) from the International Space Station (ISS). The SARJ analysis was difficult, due to the fact that the failure occurred on a platform orbiting over 220 miles/354 km miles above the Earth at approximately 17,000 miles per hour/27,359 km/hr. Evidence had to be gathered by spacewalking astronauts, brought back to Earth, and analyzed. Further inspections or repairs to damaged components would have to be carried out in orbit by other astronauts on future spacewalks. Essentially, based on a fistful of fragments gathered from an orbiting outpost, Earth-based investigators would try to determine the reason for the failure of a system in orbit.

The ISS is used for an array of scientific tests and investigations, and serves as an emergency way point for the space shuttle should an in-flight occurrence necessitate an emergency docking. The ISS was planned to be an outpost that would grow over time and has done just that, Figure 1. The ISS started out in 1998 with Russian and American segments linked.

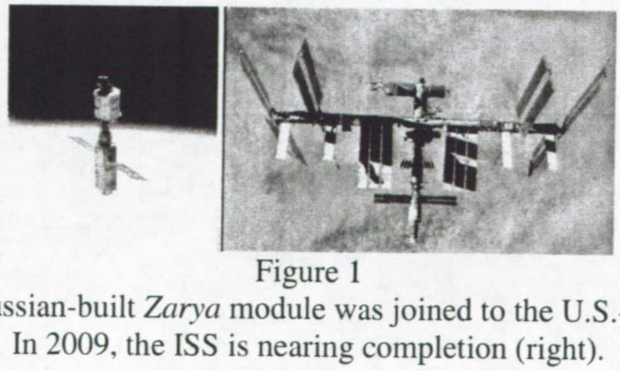

Figure 1
In 1998 (left) the Russian-built *Zarya* module was joined to the U.S.-built *Unity* module. In 2009, the ISS is nearing completion (right).

Many missions and many years later, the ISS is approaching its targeted completion date in 2011. Just as the size of the station increases, so does the list of international partners involved, which now stands at 14 countries, including the Unites States, Russia, Japan, Canada, and the members of the European Space Agency. As the construction continues, one of the most recent additions delivered to the ISS in July of 2009 aboard the space shuttle *Endeavour* during STS-127, Figure 2, was the final components of the Japanese Kibo experiment module, the largest single ISS module. NASA and the Japanese Aerospace Exploration Agency (JAXA) delivered the components over the course of three shuttle missions. As the size and capabilities of the ISS increases, so do its requirements for energy to power the various systems and equipment aboard. In order to maximize the energy that the growing station can derive from the Sun, the ISS's photovoltaic solar arrays auto-track the Sun.

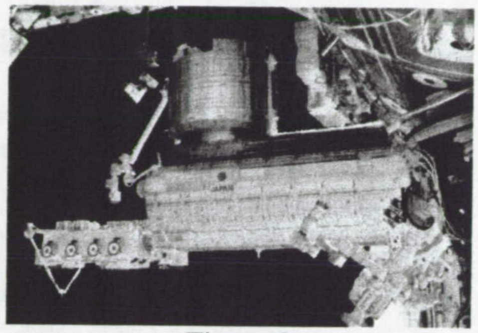

Figure 2
The Kibo Japanese Experiment Module laboratory and Exposed Facility recently deployed during STS-127.

As expansive and robust as the ISS and its scientific capabilities are, its analytical and forensic resources are limited. In order to investigate the failure of a system or component aboard the station, determine its failure mode, propose a repair, and ensure that a similar failure does not occur in the future, the logistical considerations are immense. Involved space-based failures must be investigated back on Earth, and ISS crew members must work in unison with Mission Control to coordinate any investigation. Such was the case when an anomaly was discovered with one of the mechanisms that auto-track the solar arrays with the Sun, specifically the starboard SARJ. The SARJ is essentially a 10 ft/3.05m diameter ring with two associated drive lock assemblies (DLAs) and 12 associated trundle bearing assemblies (TBAs) which travel along the SARJ, Figure 3. Gold plated 440C rollers inside the TBAs make rolling contact with the nitrided 15-5 PH stainless steel races of the SARJ; the gold plating helped serve as lubrication between the TBAs and SARJ bearing surfaces. In 2007, NASA engineers noticed an increased power draw when the starboard SARJ was operated. Likewise, higher than nominal vibration of the starboard SARJ was detected, potentially a result of excessive friction. Further analysis revealed a correlation between the vibrations and electrical demands. The starboard SARJ would need to be inspected in order to ascertain the cause of the anomalies.

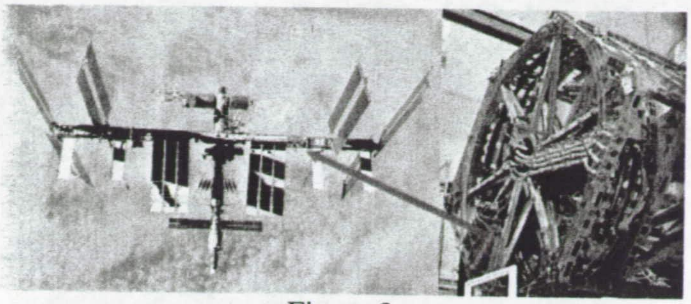

Figure 3
Starboard SARJ location aboard ISS.

Investigation
Flight engineer Dan Tani performed a spacewalk, referred to as an extra-vehicular activity (EVA), during shuttle mission STS-120. One of the objectives of the EVA was to inspect the starboard SARJ, Figure 4, and determine the cause of the electrical and vibrational anomalies.

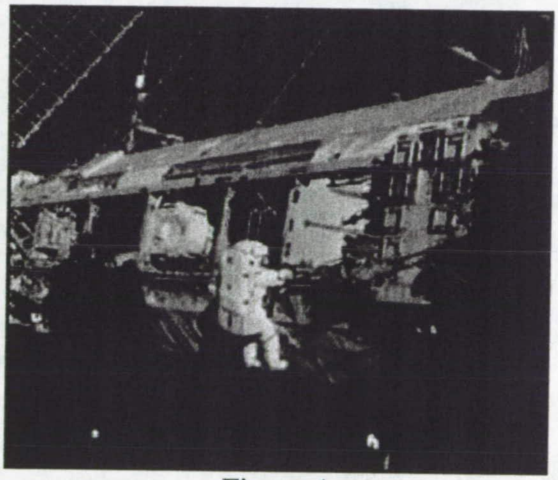

Figure 4
Astronaut Dan Tani, Expedition 16 flight engineer, harvesting debris from the SARJ.

During this and subsequent EVAs, as Dan Tani removed insulation covers protecting the SARJ and its hardware, he found that the outboard raceway of the SARJ appeared mottled. The inboard race ring and gear teeth did not display similar damage. Likewise, he reported the appearance of metallic debris decorating portions of the race, particularly near TBAs 4 and 5. Areas away from the TBAs and DLAs still appeared damaged although they did not display as much contamination. After photographing the assembly, Astronaut Tani collected samples of the debris on adhesive tape for later analysis back on Earth. He replaced the covers and completed a nearly seven hour EVA. The collected samples were returned to Earth aboard the shuttle *Discovery*. Figure 5 shows the general area where damage and debris was observed, along with a larger picture of the debris area.

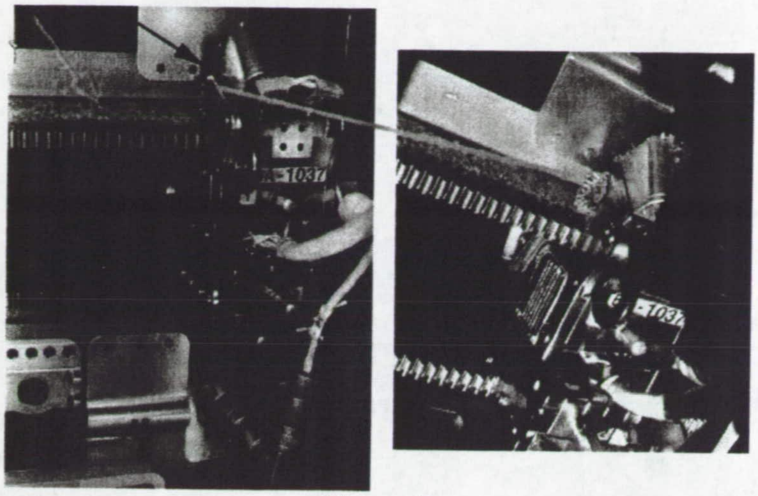

Figure 5
Section of damaged outer race (red arrow) adjacent to Trundle Bearing Assembly (TBA) on starboard SARJ. Debris (black arrow) was evident adhering to TBA.

Immediately after de-stow, the tape samples were transported to the laboratory for analysis. This portion of the testing focused on identifying the debris, determining its origin, and trying to ascertain the mode of failure. Of particular interest was determining if gold was present in the debris, which would indicate that the TBA rollers were losing material, and if any non-nitrided 15-5 PH stainless steel was present, which would indicate that the mottling damage to the SARJ extended below the nitrided layer of the race. Additionally, it was hoped that surface morphology of the fragments would help identify the failure mechanism. Root cause analysis could not be performed until an actual TBA was delivered back to Earth, which did not occur until STS-122, several months later. The testing and analysis for this investigation included photodocumentation of the samples, stereomicroscopy, scanning electron microscopy (SEM) with energy dispersive spectroscopy (EDS), and confocal laser microscopy.

Following delivery to the laboratory, photography was performed to document the as-received condition of the tape samples in their protective sample bags. Specific orientation had to be maintained since each of the three tapes which were returned to Earth had several areas of samples corresponding to particular regions from which they were removed from the SARJ.

Stereomicroscopy of the debris was performed. The shavings, shards, and slivers appeared to range from powdery to small chip-like fragments. Particle size distribution for the various samples varied greatly, from less than 100 μm to greater than 1mm. Although the majority of the number of pieces of debris were less than 50 μm, the relatively few larger fragments constituted the majority of the weight and surface area of the collected debris. Many of the larger flakes displayed what appeared to be fracture surfaces, Figure 6. Some fragments also displayed a weak magnetic response in the vicinity of a magnetic field.

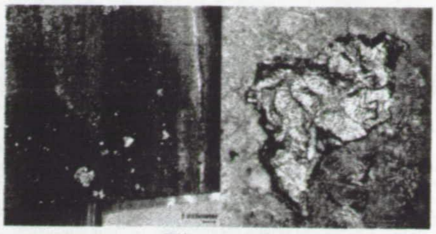

Figure 6

Typical debris with wide size distribution (left) and fracture features (right). Scale is mm.

SEM analysis identified two predominant types of debris, Figures 7 and 8: finer, apparently crushed debris, and larger, relatively intact flakes. While much of the finer debris appeared compacted and agglomerated, several of the larger fragments still had original machine marks intact, indicating that they had not yet been pulverized. Incipient spalling was apparent on the machined surfaces of one of the larger flakes examined. The reverse of this flake showed original fracture features which had not been obliterated, including scalloping and crack arrest marks, typical of spalling via contact stress fatigue with subsurface initiation. Brittle features such as cleavage steps perpendicular to primary fracture surfaces and cleavage feathering were also observed.

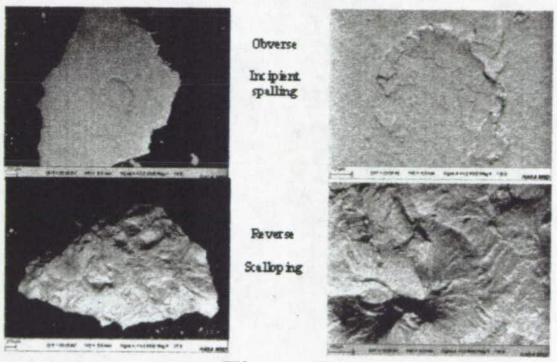

Figure 7

Incipient spalling (obverse) and scalloping and crack arrest features (reverse). Fractograph magnifications: 29X, 115X (upper left, right); 27X, 134X (lower left, right)

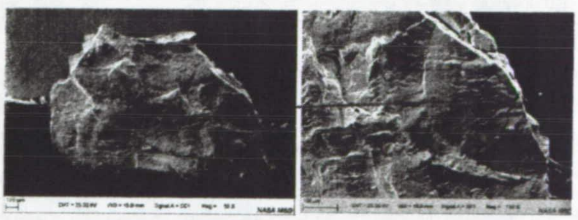

Figure 8

Fractograph depicting intact fracture surface (left) displaying initiation site, propagation region, and crack arresting (right). Original magnifications: 50X (left), 150X (right)

The samples were examined via EDS, Figure 9. The majority of debris of all sizes was composed of nitrided 15-5 PH stainless steel; no base 15-5 PH stainless steel was detected. Further, the lack of fluorine verified that no fluorinated lubricant was present. Additionally, gold particles and silver flakes were found. Aluminum, magnesium, and calcium contamination was also revealed.

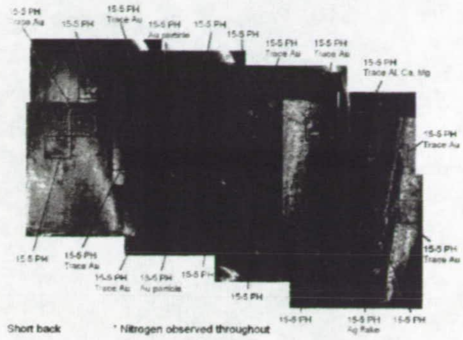

Figure 9
Representative EDS locations and compositional distribution.

Techniques, including confocal laser microscopy and metallography, were employed to measure the thickness of the fragments, which would help determine if the shards were from the non-nitrided core of the SARJ. Optical sections imaged at 100X magnification under the confocal microscope were then projected to create 2- and 3-dimensional topographical models. The thicknesses of the measured fragments ranged from 100 to 260 μm (0.004 to 0.010 inch). Metallography was employed to determine particle thickness. Representative samples were cross sectioned and prepared metallographically; typical thicknesses obtained via metallography ranged from 100 to 165 μm (0.004 to 0.006 inch). Metallography specimens also showed that even the largest fragments did not contain core or interface layer; the examined samples were from the nitrided region.

Conclusions

The samples returned to Earth were analyzed via various techniques. Particle size distribution was typically in the 100 to 260 μm (0.004 to 0.01 inch) range. Smaller particles appeared crushed and agglomerated, obliterating the evidence of their origin. Fractographic and morphological features indicated that the larger particles spalled off due to contact stress fatigue with subsurface initiation. The lack of non-nitrided 15-5 PH stainless steel indicates that the spalling was restricted to the nitrided layer of the SARJ race. The gold plating on the rollers of the TBAs was the likely source of the gold found amongst the samples. It would appear that the gold on the TBAs of the starboard SARJ did not perform as designed; the root cause determination of gold adherence was the subject of a separate, later investigation. As the gold failed on the TBA bearings, the lubricating effects of the plating became inadequate during operation, thereby increasing the friction between the rollers and races. This escalation in friction eventually caused the nitrided 15-5 PH stainless steel race to spall. The decreasing lubricity effectiveness and debris generation via spalling led to both an increase in current needed to power the system and resultant vibrations which were originally detected and initiated the investigation.

The logistics involved in performing the analysis of the SARJ failure were daunting. However, by the concerted efforts of both space-based and Earth-based personnel, a failure which occurred on the orbiting space station was able to be analyzed via a combination of spacewalks to collect the evidence, human space flight to transport the evidence, and laboratory examination to analyze the evidence.